

Where Is the Limit of Highly Fluorinated High-Oxidation-State Osmium Species?

Sebastian Riedel† and Martin Kaupp*

Institut für Anorganische Chemie, Universität Würzburg, Am Hubland, 97074 Würzburg, Germany

Received June 13, 2006

The structures and stabilities of various osmium fluorides and oxyfluorides in high oxidation states have been studied by quantum-chemical calculations at DFT (B3LYP), MP2, CCSD, and CCSD(T) levels. The calculations indicate that the homoleptic fluorides all the way up to OsF_8 may exist, even though OsF_8 will be difficult to prepare. The last missing osmium oxyfluoride, OsOF_6 , is computed to be thermochemically stable against mononuclear gas-phase elimination reactions. The problem with the nonexistence of such highly fluorinated complexes appears thus to be mainly in difficult synthetic access under typical condensed-phase conditions. Matrix-isolation techniques might provide a means to characterize the highly fluorinated Os^{VIII} and Os^{VII} species.

1. Introduction

The highest oxidation state +VIII of the 5d transition-metal osmium (in fact, of any element) is best exemplified by the tetroxide, OsO_4 , which has achieved substantial importance as an oxidation agent, for example, in organic chemistry.^{1–3} In contrast, the octafluoride, OsF_8 , is presently unknown, despite a long speculative history: In 1913, Ruff and Tschirch⁴ claimed the first synthesis of OsF_8 . Forty-five years later, Weinstock and Malm⁵ showed that the purported OsF_8 was in fact OsF_6 . The isolation of OsF_7 , reported in 1966,⁶ also could recently not be reproduced under the indicated conditions⁷ (reaction of metal powder with F_2 at 620 °C and 400 bar with subsequent rapid cooling). The highest binary osmium fluoride characterized beyond doubt is thus OsF_6 (see Figure 1).⁸

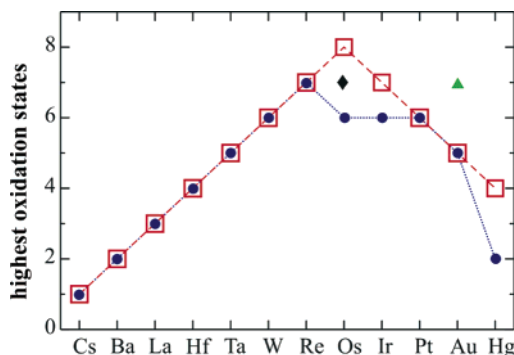


Figure 1. Maximum oxidation states of binary 5d transition-metal fluorides: (●) highest experimentally known MF_n species, (▲) incorrect experimental assignment, (◆) controversial experimental assignment, and (□) suggested maximum achievable oxidation states.

Figure 1 shows also that the decrease of the maximum oxidation states of the fluorides from group 8 through group 13 is irregular if we consider only the experimentally proven cases. Apart from OsF_8 , the lack of IrF_7 ⁹ and of HgF_4 ^{10–13} prohibits a more regular trend (earlier reports on AuF_7 have recently been shown to be erroneous¹⁴).

To investigate the chances to prepare species like OsF_8 and OsF_7 , we report here quantum-chemical calculations of

* To whom correspondence should be addressed. Fax: (+49) 931-888-7135. E-mail: kaupp@mail.uni-wuerzburg.de.

† Present address: Department of Chemistry, University of Helsinki, A.I. Virtasen aukio 1, FIN-00014 Helsinki, Finland.

- Bales, B. C.; Brown, P.; Dehestani, A.; Mayer, J. M. *J. Am. Chem. Soc.* **2005**, *127*, 2832.
- Kolb, H. C.; VanNieuwenhze, M. S.; Sharpless, K. B. *Chem. Rev.* **1994**, *94*, 2483.
- Andersson, M. A.; Epple, R.; Fokin, V. V.; Sharpless, K. B. *Angew. Chem., Int. Ed.* **2002**, *41*, 472.
- Ruff, O.; Tschirch, F. W. *Ber.* **1913**, *46*, 929.
- Weinstock, B.; Malm, J. G. *J. Am. Chem. Soc.* **1958**, *80*, 4466.
- Glemser, O.; Roesky, H. W.; Hellberg, K. H.; Werther, H. U. *Chem. Ber.* **1966**, *99*, 2652.
- Shorafa, H.; Seppelt, K. *Inorg. Chem.* **2006**, *45*, 7929.
- (a) Holleman, A. F.; Wiberg, E. *Lehrbuch der Anorganischen Chemie*, 71st–101st ed.; Walter de Gruyter: Berlin, 1995. (b) Greenwood, N. N.; Earnshaw, A. *Chemistry of the Elements*, 2nd ed.; Elsevier: Oxford, 1997.

- Riedel, S.; Kaupp, M. *Angew. Chem., Int. Ed.* **2006**, *45*, 3708.
- Riedel, S.; Straka, M.; Kaupp, M. *Phys. Chem. Chem. Phys.* **2004**, *6*, 1122.
- Riedel, S.; Straka, M.; Kaupp, M. *Chem.-Eur. J.* **2005**, *11*, 2743.
- Kaupp, M.; Dolg, M.; Stoll, H.; von Schnering, H. G. *Inorg. Chem.* **1994**, *33*, 2122.
- Kaupp, M.; von Schnering, H. G. *Angew. Chem., Int. Ed. Engl.* **1993**, *32*, 861.
- Riedel, S.; Kaupp, M. *Inorg. Chem.* **2006**, *45*, 1228.

structures and (gas-phase) stabilities. Additionally, we evaluate also the stabilities of heteroleptic Os^{VIII} oxyfluorides, to find out how they are affected by the number of fluorine atoms present. We will compare our results also to those of an earlier HF and MP2 study of osmium fluorides and oxyfluorides by Veldkamp and Frenking.¹⁵ Notably, however, those authors had to rely on various isodesmic reactions to discuss stability, whereas the more refined and advanced computational methods available today allow us to discuss directly the relevant gas-phase elimination and bond-breaking reactions, and to evaluate also activation barriers for some key reactions.

2. Computational Methods

Structures were optimized using density-functional theory (hybrid B3LYP^{16–19} functional), with the Gaussian 03¹⁶ program. The transition-state optimizations were done using synchronous transit-guided quasi-newton (STQN) methods^{20,21} according to the QST2 and QST3 keywords implemented in Gaussian 03. Optimizations were followed by single-point energy calculations at DFT, MP2, and high-level coupled-cluster (CCSD and CCSD(T)) levels. Quasirelativistic energy-adjusted, small-core “Stuttgart-type” pseudopotentials (effective-core potentials, ECPs) were used for the transition metals Os,²² Au,²² Pt,²² and Ir.²² The corresponding (8s7p6d)[6s5p3d] valence basis sets were augmented by one f-type polarization function²³ (exponent α : Os 0.886, Ir 0.938, Pt 0.993, and Au 1.050). Energy-adjusted 8-valence-electron pseudopotentials and (6s6p3d1f)/[4s4p3d1f] valence basis sets were used for the noble-gas atoms Ng = Kr, Xe.²⁴

In the B3LYP-optimizations, a fluorine DZ+P all-electron basis set by Dunning²⁵ was used. Stationary points on the potential energy surface were characterized by harmonic vibrational frequency analyses at this level (providing also zero-point energy corrections to the thermochemistry). The subsequent single-point energy calculations had the fluorine basis replaced by a larger aug-cc-

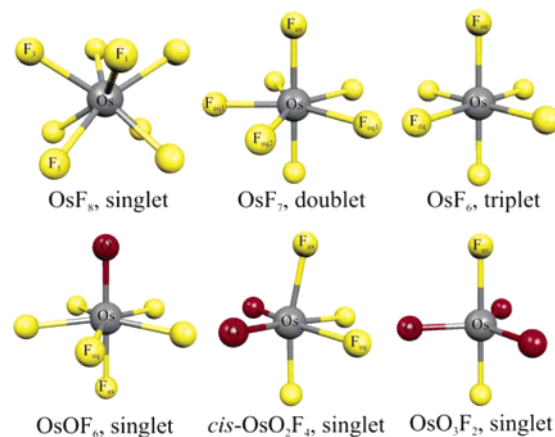


Figure 2. B3LYP-optimized minimum structures of OsF₈ (*D*_{4d}), OsF₇ (*C*_{2v}), OsF₆ (*D*_{4h}), OsOF₆ (*C*_{5v}), *cis*-OsO₂F₄ (*C*_{2v}), and OsO₃F₂ (*D*_{3h}). Distances and angles are in Table 1.

pVTZ basis set.²⁶ The post-HF calculations were carried out with the MOLPRO 2002.6²⁷ program package. Basis-set superposition errors (BSSE) were estimated by the counterpoise (CP)^{28,29} procedure. We note that the methodology used here, in particular B3LYP optimizations followed by B3LYP or CCSD(T) single-point energy calculations with larger basis sets, is well established as a reliable tool for redox thermochemistry in the 5d transition-metal series, for example, in previous studies on Hg, Au, Pt, and Ir systems.^{9,10,14} We have furthermore found excellent agreement with structures and relevant thermochemical data in test calculations on ReF₇ (the results will be reported elsewhere as part of a wider computational study on technetium and rhenium fluorides). We do not consider spin-orbit corrections in this work. Our previous studies indicated spin-orbit effects to have only a minor influence on the relevant thermochemical data or activation barriers, even when open-shell 5d species were involved.⁹

3. Results and Discussion

Figure 2 shows the B3LYP-optimized structures of OsF₈, OsF₇, and OsF₆. At this computational level, we find two minima for OsF₈. One is a distorted quadratic antiprism with *D*_{2d} symmetry and two different Os–F bonds (Table 1). The other is a regular quadratic antiprism with *D*_{4d} symmetry. The energies of the two minima differ only by less than 5 kJ mol^{–1}, and the calculations suggest a shallow potential energy surface around the two located minima. An earlier study at HF and MP2 levels indicated a pronounced dependence on computational method. At HF level (with a valence DZP basis for fluorine), a more distorted *C*_{2v} structure was obtained, whereas the less distorted antiprism of *D*_{2d} symmetry was found at MP2 level. OsF₈ may indeed be a fluxional species.

- (15) Veldkamp, A.; Frenking, G. *Chem. Ber.* **1993**, *126*, 1325.
 (16) Frisch, M. J.; Trucks, G. W.; Schlegel, H. B.; Scuseria, G. E.; Robb, M. A.; Cheeseman, J. R.; Montgomery, J. A.; Vreven, J. T.; Kudin, K. N.; Burant, J. C.; Millam, J. M.; Iyengar, S. S.; Tomasi, J.; Barone, V.; Mennucci, B.; Cossi, M.; Scalmani, G.; Rega, N.; Petersson, G. A.; Nakatsuji, H.; Hada, M.; Ehara, M.; Toyota, K.; Fukuda, R.; Hasegawa, J.; Ishida, M.; Nakajima, T.; Honda, Y.; Kitao, O.; Nakai, H.; Klene, M.; Li, X.; Knox, J. E.; Hratchian, H. P.; Cross, J. B.; Adamo, C.; Jaramillo, J.; Gomperts, R.; Stratmann, R. E.; Yazyev, O.; Austin, A. J.; Cammi, R.; Pomelli, C.; Ochterski, J. W.; Ayala, P. Y.; Morokuma, K.; Voth, G. A.; Salvador, P.; Dannenberg, J. J.; Zakrzewski, V. G.; Dapprich, S.; Daniels, A. D.; Strain, M. C.; Farkas, O.; Malick, D. K.; Rabuck, A. D.; Raghavachari, K.; Foresman, J. B.; Ortiz, J. V.; Cui, Q.; Baboul, A. G.; Clifford, S.; Cioslowski, J.; Stefanov, B. B.; Liu, G.; Liashenko, A.; Piskorz, P.; Komaromi, I.; Martin, R. L.; Fox, D. J.; Keith, T.; Al-Laham, M. A.; Peng, C. Y.; Nanayakkara, A.; Challacombe, M.; Gill, P. M. W.; Johnson, B.; Chen, W.; Wong, M. W.; Gonzalez, C.; Pople, J. A. *Gaussian 03*, revision B.04; Gaussian, Inc.: Pittsburgh, PA, 2003.
 (17) Becke, A. D. *J. Chem. Phys.* **1993**, *98*, 5648.
 (18) Lee, C.; Yang, W.; Parr, R. G. *Phys. Rev. B* **1988**, *37*, 785.
 (19) Miehlisch, B.; Savin, A.; Stoll, H.; Preuss, H. *Chem. Phys. Lett.* **1989**, *157*, 200.
 (20) Peng, C.; Schlegel, H. B. *Isr. J. Chem.* **1994**, *33*, 449.
 (21) Peng, C.; Ayala, P.; Schlegel, H. B.; Frisch, M. J. *J. Comput. Chem.* **1996**, *17*, 49.
 (22) Andrae, D.; Häussermann, U.; Dolg, M.; Stoll, H.; Preuss, H. *Theor. Chim. Acta* **1990**, *77*, 123.
 (23) Ehlens, A. W.; Bohme, M.; Dapprich, S.; Gobbi, A.; Hollwarth, A.; Jonas, V.; Kohler, K. F.; Stegmann, R.; Veldkamp, A.; Frenking, G. *Chem. Phys. Lett.* **1993**, *208*, 111.
 (24) Nicklass, A.; Dolg, M.; Stoll, H.; Preuss, H. *J. Chem. Phys.* **1995**, *102*, 8942.
 (25) Dunning, T. H., Jr. *J. Chem. Phys.* **1970**, *53*, 2823.

- (26) Dunning, T. H., Jr. *J. Chem. Phys.* **1989**, *90*, 1007.
 (27) Werner, H.-J.; Knowles, P. J.; Lindh, R.; Schütz, M.; Celani, P.; Korona, T.; Manby, F. R.; Rauhut, G.; Amos, R. D.; Bernhardsson, A.; Berning, A.; Cooper, D. L.; Deegan, M. J. O.; Dobbyn, A. J.; Eckert, F.; Hampel, C.; Hetzer, G.; Lloyd, A. W.; McNicholas, S. J.; Meyer, W.; Mura, M. E.; Nicklass, A.; Palmieri, P.; Pitzer, R.; Schumann, U.; Stoll, H.; Stone, A. J.; Tarroni, R.; Thorsteinsson, T. *MOLPRO 2002.6 a package of ab initio programs*; MOLPRO 2002.6: Birmingham, UK, 2003.
 (28) Boys, S. F.; Bernardi, F. *Mol. Phys.* **1970**, *19*, 553.
 (29) Simon, S.; Duran, M.; Dannenberg, J. J. *J. Chem. Phys.* **1996**, *105*, 11024.

Table 1. Experimental and B3LYP-Optimized Minimum Structures^a

species	symmetry	species	symmetry	species	symmetry
OsF ₈	<i>D</i> _{2d} (<i>D</i> _{4d}) ^b	OsF ₇	<i>C</i> _{2v}	OsF ₆ ^c	<i>D</i> _{4h}
Os–F ₁	186.7 (188.2)	F _{ax}	183.9	F _{ax}	185.8
Os–F ₃	189.9 (188.2)	F _{eq1}	185.6	F _{eq}	184.0
Os–F ₅	1.867 (188.2)	F _{eq2}	189.0		
F ₁ –Os–F ₂	104.0 (114.3)	F _{eq3}	186.9		
F ₃ –Os–F ₄	123.8 (114.3)	F _{eq1} –Os–F _{eq2}	71.9		
F ₁ –Os–F ₅	86.4 (78.2)	F _{eq2} –Os–F _{eq3}	72.2		
		F _{eq3} –Os–F _{eq4}	71.8		
OsOF ₆	<i>C</i> _{5v}	<i>cis</i> -OsO ₂ F ₄	<i>C</i> _{2v}	OsO ₃ F ₂	<i>D</i> _{3h}
Os–O	167.8	Os–F _{ax}	186.1	Os–F _{ax}	189.3
Os–F _{eq}	188.6	Os–O	169.0	Os–O	169.7
Os–F _{ax}	186.1	Os–F _{eq}	188.8		
O–Os–F _{eq}	93.6	F _{ax} –Os–O	93.9		
F _{eq} –Os–F _{eq}	71.8	F _{ax} –Os–F _{eq}	85.3		
		F _{ax} –Os–F _{ax}	167.8		

^a Distances in picometers and angles in degrees. See Figure 1 for atom numbering. ^b Values in parentheses are for the *D*_{4d} minimum; see text. ^c Experimental (X-ray single-crystal study)³⁹ bond lengths of OsF₆ are Os–F_{ax1} 183.33(24), Os–F_{eq1} 182.21(18), Os–F_{ax2} 182.80(25), Os–F_{eq2} 182.92(18). ^d Experimental bond lengths of OsO₂F₄ from gas-phase electron diffraction³⁵ are Os–O 167.4(4), Os–F_{ax} 184.3(3), Os–F_{eq} 188.3(3).

Table 2. Computed Reaction Energies (in kJ mol^{−1})^a

reaction	B3LYP	MP2	CCSD	CCSD(T)
(a) OsF ₈ → OsF ₆ + F ₂ ^b	−79.1 (−97.3)	63.0	−150.8	−73.1
(b) OsF ₈ → OsF ₇ + F ^b	6.6 (−7.8)	94.2	−38.4	14.4
(c) OsF ₇ → OsF ₅ + F ₂ ^b	218.9 (206.8)	303.7	108.7	186.5
(d) OsF ₇ → OsF ₆ + F ^b	69.6 (59.5)	142.4	12.0	65.2
(e) OsF ₆ → OsF ₅ + F ^b	304.6 (296.4)	334.9	221.1	274.1
(f) OsF ₆ + KrF ₂ → OsF ₈ + 2Kr	43.4	−91.6	65.8	12.2
(g) OsF ₅ + KrF ₂ → OsF ₇ + 2Kr	−254.6	−332.2	−193.7	−247.4
(h) [OsF ₆] [−] + [KrF] ⁺ → OsF ₇ + Kr ^c	−688.7	−746.3	−552.7	−633.5
(i) OsOF ₆ → OsOF ₄ + F ₂	138.7	298.2	158.7	133.6
(j) OsOF ₆ → OsF ₅ + OF	170.3	507.4	116.2	233.7
(k) OsOF ₆ → OsF ₆ + O	97.5	390.0	73.7	164.7
(l) OsOF ₆ → OsOF ₅ + F	54.2	150.1	4.1	54.8
(m) OsO ₂ F ₄ + 2F ₂ → OsF ₈ + O ₂	−205.6	−129.2	−104.8	−110.2
(n) OsO ₂ F ₄ + 2KrF ₂ → OsF ₈ + 2Kr + O ₂	−276.9	−186.3	−274.8	−232.1
(o) OsO ₄ + 4KrF ₂ → OsF ₈ + 4Kr + 2O ₂	−836.9	−711.9	−921.3	−805.0
(p) OsO ₄ + 2KrF ₂ → OsO ₂ F ₄ + 2Kr + O ₂	−560.0	−525.7	−646.5	−572.9
(q) OsO ₂ F ₄ + KrF ₂ → OsOF ₆ + Kr + O	96.7	95.0	28.6	71.5
(r) OsO ₂ F ₄ + F ₂ → OsOF ₆ + O	132.4	123.5	113.7	132.4
(s) OsO ₂ F ₄ + 2F ₂ → OsOF ₆ + OF + F	55.9	79.6	59.5	80.1
(t) OsO ₃ F ₂ + 2F ₂ → OsOF ₆ + O ₂	−473.3	−387.2	−348.1	−337.9
(u) KrF ₂ → Kr + F ₂ ^d	−35.7	−28.5	−85.0	−60.9
(v) F ₂ → 2F ^e	155.3	173.6	124.4	152.7

^a Reaction energies for singlet OsF₈, doublet OsF₇, triplet OsF₆, quartet OsF₅, singlet OsOF₆, singlet OsO₂F₄, singlet OsO₃F₂, and singlet OsO₄. ^b Values in parentheses are counterpoise and zero-point vibration corrected. ^c Energies for the separate steps are: (i) formation of the ion-pair complex −545.2 kJ mol^{−1}, and (ii) decomposition to OsF₇ and Kr −143.5 kJ mol^{−1} (B3LYP result). ^d The experimental value is −60.2 ± 3.4 kJ mol^{−1}.^{40,41} ^e The experimental value is +158.3 kJ mol^{−1}.^{42,43}

Unimolecular gas-phase F₂-elimination from OsF₈ to give OsF₆ is found to be exothermic (see Table 2, reaction a). However, the computed barrier for concerted elimination at B3LYP level is appreciable, 203.9 kJ mol^{−1}. The transition state has *C*_{2v} symmetry. A second potential channel for decomposition of OsF₈ involves the homolytic dissociation of an Os–F bond to give OsF₇. This reaction is endothermic (by 14.4 kJ mol^{−1} at CCSD(T) level; Table 2, reaction b) and exhibits an appreciable barrier of 144.0 kJ mol^{−1}, due to substantial nuclear reorganization. Bimolecular F₂-elimination to give OsF₇ (Table 3, reaction a) is strongly exothermic and may be a reason why OsF₈ has not been observed in typical condensed-phase reactions (computation of activation barriers of bimolecular reaction channels is outside the scope of the present work).

We note in passing the good agreement between B3LYP and CCSD(T) thermochemistry, whereas MP2 tends to

overestimate and CCSD tends to underestimate the stabilities of the high-oxidation-state species significantly. These trends are consistent with appreciable differential nondynamical correlation effects and agree with our earlier experience on redox reactions of 5d transition-metal fluoride complexes.^{9,10,12–14} We consider the B3LYP and CCSD(T) results to provide faithful estimates of the reaction energies. The good performance of B3LYP in this field of 5d-metal fluoride redox reactions (as compared to pure gradient-corrected functionals or hybrid functionals with larger exact-exchange admixtures^{9,10,14}) is notable also in view of an apparently nonuniform quality of B3LYP in other areas of transition-metal thermochemistry.³⁰

Moving to the next lower homoleptic fluoride, we find OsF₇ to exhibit a (doublet state) minimum with *C*_{2v} symmetry

(30) Furche, F.; Perdew, J. P. *J. Chem. Phys.* **2006**, *124*, 044103/1.

Table 3. Computed Bimolecular Decomposition Reactions (in kJ mol⁻¹)^a

reaction	B3LYP	MP2	CCSD	CCSD(T)
(a) 2OsF ₈ → 2OsF ₇ + F ₂	-142.0	3.4	-212.2	-131.9
(b) 2OsF ₇ → 2OsF ₆ + F ₂	-16.1	111.3	-100.4	-22.4
(c) 2OsF ₆ → 2OsF ₅ + F ₂	453.9	496.1	317.7	395.4
(d) 2OsOF ₆ → 2OsF ₆ + O ₂	-319.6	200.4	-295.5	-151.1
(e) 2OsOF ₆ → 2OsOF ₅ + F ₂	-46.9	126.7	-116.2	-43.1
(f) 2OsO ₂ F ₄ + 2F ₂ → 2OsOF ₆ + O ₂	-249.7	-332.7	-215.6	-215.7
(g) 2OsO ₂ F ₄ + 2KrF ₂ → 2OsOF ₆ + O ₂ + 2Kr	-321.1	-389.7	-385.6	-337.5
(h) 2OsF ₆ + KrF ₂ → 2OsF ₇ + Kr	-19.5	-139.8	15.4	-38.6

^a See footnote 1 to Table 2.**Table 4.** Computed Adiabatic First Ionization Potentials (in eV) of Neutral Osmium Fluoride Complexes and Decomposition Reaction Energies of Cationic Species (in kJ mol⁻¹)^a

reaction	B3LYP	MP2	CCSD	CCSD(T)
(a) OsF ₇ → [OsF ₇] ⁺	12.6	11.4	13.3	12.5
(b) OsOF ₅ → [OsOF ₅] ⁺	12.3	11.1	12.8	12.2
(c) [OsF ₇] ⁺ → [OsF ₆] ⁺ + F	32.3	128.1	-24.5	33.5
(d) [OsF ₇] ⁺ → [OsF ₅] ⁺ + F ₂	88.3	257.9	-36.3	76.7
(e) [OsOF ₅] ⁺ → [OsOF ₄] ⁺ + F	116.6	245.2	34.7	114.5
(f) [OsOF ₅] ⁺ → [OsOF ₃] ⁺ + F ₂	277.7	469.4	185.1	279.6

^a Reaction energies for doublet OsF₇, singlet [OsF₇]⁺, doublet [OsF₆]⁺, triplet [OsF₅]⁺, doublet OsOF₅, singlet [OsOF₅]⁺, doublet [OsOF₄]⁺, and triplet [OsOF₃]⁺.

(Figure 2). Unimolecular F₂-elimination, OsF₇ → OsF₅ + F₂, is now appreciably endothermic (by 186.5 kJ mol⁻¹ at CCSD(T) level, Table 2). Homolytic bond cleavage costs 65.2 kJ mol⁻¹ at the same level, with a relatively high barrier of 237.0 kJ mol⁻¹, due to extensive nuclear reorganization (B3LYP result). These results suggest appreciable stability for OsF₇ under typical gas-phase conditions. Notably, however, the bimolecular F₂-elimination (Table 3, reaction b) is exothermic. The characterization of OsF₇ in ref 6 was mainly based on an IR spectrum that differed from that of OsF₆. Our computed vibrational spectra (Table 5) suggest substantial differences between the two species but do not agree too well with the reported solid-state data on OsF₇. A recent attempt by Shorafa and Seppelt⁷ to reproduce the reaction of ref 6 gave pure OsF₆ as sole product, as indicated by low-temperature Raman spectroscopy. Our computations do not allow us to interpret the experimental results of ref 6 at this point. In any case, OsF₇ appears to be a clearly more stable species and more easily accessible target (at least in gas-phase or matrix-isolation experiments) as compared to OsF₈. It is doubtful, however, whether the high-temperature condensed-phase conditions employed in the experiments would allow isolation of such a highly reactive species.

Previous attempts to prepare the higher homoleptic fluorides (OsF₇, OsF₈) by fluorinating OsOF₅ with KrF₂ have been unsuccessful, as neither oxygen elimination nor fluorination were observed.³¹ Table 2 includes a number of reactions involving KrF₂ and KrF⁺, as well as some isoelectronic xenon compounds. The oxidation reaction OsF₆ + KrF₂ → OsF₈ + Kr is calculated to be slightly endothermic (Table 2, reaction f). This indicates that preparation of OsF₈ will indeed be a great challenge. In contrast, oxidation of

OsF₅ (Table 2, reaction g) or of OsF₆ (Table 3, reaction h) by KrF₂ is substantially exothermic. This holds even more so for the strongest presently known oxidative fluorinating agent KrF⁺.³² Formation of the [KrF][OsF₆] ion-pair from (gas-phase) [KrF]⁺ and quartet [OsF₆]⁻ is highly exothermic (-545.2 kJ mol⁻¹ at B3LYP level) and provides a local minimum on the potential energy surface. However, [KrF]-[OsF₆] is calculated to decompose exothermically (by -143.5 kJ mol⁻¹) into OsF₇ and Kr. Reaction of the related [XeF]-[OsF₆] is calculated to be endothermic (experimentally, this ion-pair complex decomposes at 20 °C according to 3[XeF][OsF₆] → [Xe₂F₃][OsF₆] + 2OsF₆ + Xe³³).

Figure 3 shows the reaction energies [NgF][MF₆] → MF₇ + Ng for a range of ion pairs (Ng = Kr, Xe and M = Os, Ir, Pt, Au) at the corresponding computational level (note that these energies will be generally somewhat more positive in the condensed phase due to electrostatic stabilization of the ion-pair complexes). Reaction of [KrF][IrF₆] to give IrF₇ is also exothermic and has recently been suggested as a possible pathway toward Ir^{VII}.⁹ Figure 3 suggests analogous access to OsF₇. Interestingly, in contrast to several known [KrF][MF₆] complexes of platinum and gold, and despite the existence of [XeF][IrF₆],³³ the corresponding osmium [NgF][OsF₆] and [KrF][IrF₆] complexes have never been observed.

Veldkamp and Frenking¹⁵ had discussed isodesmic fluorination reactions of Os^{VIII} oxofluorides as a possible pathway toward OsF₈. Unfortunately, experimental investigations suggest that these types of fluorinations, either with F₂ or with KrF₂, stop at the known OsO₂F₄ stage,³⁴⁻³⁶ and further fluorination is unsuccessful. Thus, even OsOF₆ is not known (and a structure could not be located at HF or MP2 level in ref 15). Most likely, the reason is the increasing steric hindrance in the Os coordination sphere, leading to an increasing oxidizing power along the series OsO₄ < OsO₃F₂ < OsO₂F₄.³⁷ Interestingly, our computations (B3LYP or CCSD(T), Table 2) indicate exothermic fluorination, both with F₂ and with KrF₂, up to and including OsF₈ as product. Maybe the kinetics of these reactions are unfavorable (this

(32) Christe, K. O.; Dixon, D. A. *J. Am. Chem. Soc.* **1992**, *114*, 2978.(33) Sladky, F. O.; Bulliner, P. A.; Bartlett, N. *J. Chem. Soc. A* **1969**, *14*, 2179.(34) Christe, K. O.; Bougon, R. *J. Chem. Soc., Chem. Commun.* **1992**, 1056.(35) Christe, K. O.; Dixon, D. A.; Mack, H. G.; Oberhammer, H.; Pagelot, A.; Sanders, J. C. P.; Schrobilgen, G. J. *J. Am. Chem. Soc.* **1993**, *115*, 11279.(36) Bougon, R.; Ban, B.; Seppelt, K. *Chem. Ber.* **1993**, *126*, 1331.(37) Gerken, M.; Schrobilgen, G. J. Osmium(VIII) oxide and oxide fluoride chemistry. *Inorganic Chemistry in Focus II*; Wiley-VCH: Weinheim, 2005; p 243.(31) Bougon, F.; Cicha, W. V.; Isabay, J. *J. Fluorine Chem.* **1994**, *67*, 271.

Table 5. Experimental and Computed Fundamental Vibrational Frequencies (with IR and Raman Intensities) for OsF₇ and OsF₆^a

	exp. IR freq. (solid-state)	exp. IR freq. (gas-phase)	exp. Raman freq.	comp. freq.	comp. IR inten.	comp. Raman activities
OsF ₇	282			67		9
	336			193	9	
	366			268		4
	483			293	21	21
	550			303		4
	715			346	20	
				481		9
				500		4
				648		13
				661	150	
				680	150	
				706		46
				722	186	
	OsF ₆	628	268	252	159	4
700		728	632	204		4
			733	270	16	
				285		4
				468		11
				709	207	
				723		42

^a Frequencies in cm⁻¹, computed IR-intensities in km mol⁻¹, computed Raman scattering activities in A⁴ amu⁻¹. Experimental solid-state data for OsF₇ from ref 6 and for OsF₆ from ref 44. Gas-phase data for OsF₆ from ref 45.

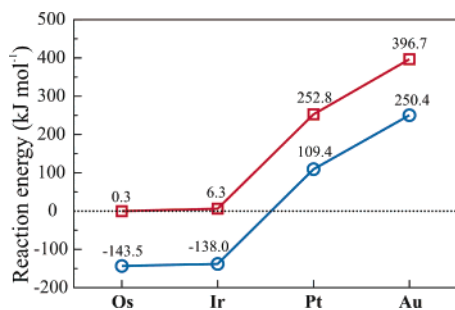


Figure 3. Computed energies (B3LYP in kJ mol⁻¹ for the (gas-phase) reactions [NgF]⁺[MF₆]⁻ → MF₇ + Ng (Ng = Kr, Xe; M = Os, Ir, Pt, Au): (□) XeF⁺ complexes, (○) KrF⁺ complexes.

will be subject of future studies). Experimental evidence suggests in any case that homoleptic lower osmium fluorides provide a better starting point for the synthesis of the higher fluorides than do the Os^{VIII} oxyfluorides.

All attempts to synthesize the highest oxyfluoride OsOF₆ were unsuccessful (a claimed preparation was later shown to have led to OsO₂F₄^{34,38}), and even the computational search for this complex failed.¹⁵ In contrast to that older computational study, we have been able to locate a minimum for OsOF₆ at B3LYP level (a similar structure is obtained at HF or MP2 levels), a pentagonal bipyramidal structure (C_{5v} symmetry, Figure 2; a monocapped octahedral C_{3v} structure is a transition state at 61.6 kJ mol⁻¹, and the monocapped

trigonal prism of C_{2v} symmetry is a second-order saddle point at 110.2 kJ mol⁻¹ above the C_{5v} minimum). All unimolecular gas-phase decomposition channels of OsOF₆ are endothermic (Table 2), including homolytic Os–F bond-breaking to give OsOF₅ (doublet), or Os–O bond cleavage to give OsF₆ (triplet). Inclusion of bimolecular channels leads to exothermic decomposition pathways (Table 3, reactions d,e). As for OsF₈ or OsF₇, this suggests gas-phase or matrix-isolation techniques as preferred tools for the preparation of OsOF₆.

The cations [OsF₇]⁺ and [OsOF₅]⁺ are of particular interest as potential precursors for the missing targets OsF₈ and OsOF₆. Singlet [OsF₇]⁺ exhibits a slightly compressed pentagonal bipyramidal structure (Os–F_{ax} 180.0 pm, Os–F_{eq} 184.7 pm). The adiabatic ionization potential OsF₇ → [OsF₇]⁺ is calculated to be appreciable at 12.5 eV (CCSD-(T) result). Os–F bond homolysis and concerted F₂-elimination are computed to be endothermic (Table 4). [OsOF₅]⁺ exhibits C_{4v} symmetry. Because of the trans influence of the oxo ligand, the axial Os–F bond is somewhat lengthened (Os–O 167.5 pm, Os–F_{ax} 183.9 pm, and Os–F_{eq} 181.2 pm). Unimolecular decomposition channels for this cation are all computed to be endothermic.

4. Conclusions

The evaluation of structures and stabilities of higher fluorides and oxyfluorides of osmium indicates that OsF₇ is a viable target for preparation. Yet, in view of potential exothermic bimolecular decomposition pathways, this might be better achieved in a gas-phase or matrix-isolation experiment than in an earlier⁶ direct condensed-phase fluorination experiment that has recently been put into question.⁷ OsF₈ is much less stable thermochemically but appears to exhibit appreciable activation barriers for its unimolecular decomposition pathways. Its experimental observation under matrix-isolation conditions appears thus also possible. The last missing Os^{VIII} oxyfluoride, OsOF₆, is even somewhat more

- (38) Bougon, R. *J. Fluorine Chem.* **1991**, *53*, 419.
 (39) Drews, T.; Supel, J.; Hagenbach, A.; Seppelt, K. *Inorg. Chem.* **2006**, *45*, 3782.
 (40) Gunn, S. R. *J. Phys. Chem.* **1967**, *71*, 2934.
 (41) Lehmann, J. F.; Mercier, H. P. A.; Schrobilgen, G. J. *Coord. Chem. Rev.* **2002**, *233–234*, 1.
 (42) Huber, K. P.; Herzberg, G. *Molecular Spectra and Molecular Structure 4: Constants of Diatomic Molecules*; Van Nostrand Rheingold: New York, 1979.
 (43) Forslund, L. E.; Kaltsoyannis, N. *New J. Chem.* **2003**, *27*, 1108.
 (44) Hellberg, K. H.; Mueller, A.; Glemser, O. *Z. Naturforsch., B: Anorg. Chem., Org. Chem., Biochem., Biophys., Biol.* **1966**, *21*, 118.
 (45) Weinstock, B.; Claassen, H. H.; Malm, J. G. *J. Chem. Phys.* **1960**, *32*, 181.

stable against unimolecular decomposition. Overall, the highest fluorides and oxyfluorides do thus remain interesting challenges for matrix-isolation spectroscopists, or possibly for mass spectrometrical identification in the gas phase, whereas classical condensed-phase syntheses appear difficult.

Acknowledgment. We are grateful to K. Seppelt for a copy of ref 7 prior to publication and for stimulating discussions. B. Engels and S. Schlund kindly provided computational resources.

IC061054Y